PRAMANA
— journal of
physics

Vol. 61, No. 5
November 2003
pp. 1027–1032

Radial, sideward and elliptic flow at AGS energies

P K SAHU[1,2] and A OHNISHI[2]
[1]Institute of Physics, Sachivalaya Marg, Bhubaneswar 751 005, India
[2]Division of Physics, Graduate School of Science, Hokkaido University, Sapporo 060-0810, Japan

Abstract. We study the baryon transverse in-plane (sideward) and elliptic flow from SIS to AGS energies for Au+Au collisions in a relativistic dynamical simulation model that includes all baryon resonances up to a mass of 2 GeV as well as string degrees of freedom for the higher mass continuum. There are two factors which dominantly determine the baryon flow at these energies: the momentum dependence of the scalar and vector potentials and the resonance-string degrees of freedom. We fix the explicit momentum dependence of the nucleon–meson couplings of NL3(hard) equation of state (EoS) by the nucleon optical potential up to 1 GeV of kinetic energy. We simultaneously reproduce the sideward flow, the elliptic flow and the radial transverse mass distribution of protons data at AGS energies. In order to study the sensitivity of different mean-field EoS, we use NL2(soft) and NL23(medium) along with NL3(hard) momenta-dependent mean-field EoS. We find that to describe data on both sideward and elliptic flow, NL3 model is better at 2 A·GeV, while NL23 model is at 4–8 A·GeV.

Keywords. Heavy-ion collisions; radial; sideward; elliptic flow.

PACS Nos 25.75.+r, 24.10.Jv

1. Introduction

When two heavy nuclei (Au+Au) collide with each other with relativistic beam energies, a large number of particles are produced. The collective motion of these particles is called flow: the radial flow, the sideward flow and the elliptic flow. The last two flows are important, because they give good insight into understanding the high-density nuclear matter, created in the heavy-ion collision experiments. Also, these give a better understanding of nuclear EoS as well as quark–gluon plasma formation, since these are produced at the early stage of collisions and hence depend on the early pressure gradient in the collisions.

The sideward flow is a deflection of forward and backward moving particles away from the beam axis within the reaction plane. This flow has more potential than radial flow in the determination of EoS, because in the transport model, it has been observed directly that the production of sideward flow is shifted towards the high-density phase. On the other hand, the elliptic flow is equally important at very high energies. Specially at SIS to AGS energies, the elliptic flow is generated from the early squeeze-out of compressed matter and particles try to move out in the direction perpendicular to the reaction plane. The elliptic flow has two signs: the negative out-of plane elliptic flow contribution comes from the squeeze-out and the positive elliptic flow indicates an in-plane enhancement. The latter one is seen at higher AGS energies and results from the asymmetric shape of the

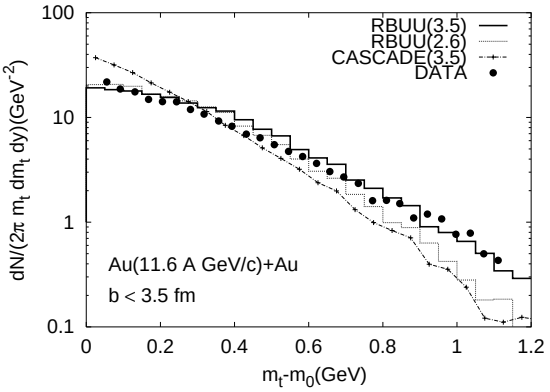

Figure 1. The solid line and the dot–dashed line with crosses are the proton transverse mass spectra for $\sqrt{s} = 3.5$ GeV with and without nuclear potentials, respectively. The dotted line is for $\sqrt{s} = 2.6$ GeV. The data points are taken from the E802 Collaboration.

overlap volume of the two nuclei. The elliptic flow may play a more crucial role in the determination of EoS than sideward flow, because it involves almost no opposition to stream of matter moving past each other since its motion is out-of reaction plane. In recent years, both the directed sideward flow and the elliptic flow have been measured [1] for heavy-ion (Au+Au) collisions at AGS energies in the incident energy range of 1 A·GeV $\leq E_{\rm inc} \leq$ 11 A·GeV. Very recently, also differential flow data are available from the E895 Collaboration [2] which allow for more severe constraints on the EoS.

Here, we study the sideward and elliptic flow of nucleons for various nucleus–nucleus collisions as a function of beam energy from 0.5 A·GeV to 11 A·GeV employing a relativistic transport model with a 'hard' EoS based on momentum-dependent scalar and vector self energies for the nucleons. However, we continue our calculations within the same transport approach using, furthermore, different EoS with incompressibilities of 210 MeV (soft) and 300 MeV (medium) along with 380 MeV (hard) as a function of beam energies.

In §2 we briefly describe the relativistic transport model and the parameter sets for the scalar and vector self energies in comparison with the 'experimental' optical potential from ref. [3]. We will systematically study the flows for Au+Au collisions from 5–8 A·GeV and discuss the results in §3. Section 4 concludes with a summary.

2. Description of the model

In this calculation we perform a theoretical analysis along the line of the relativistic transport approach RBUU which is based on a coupled set of covariant transport equations for the phase-space distributions of a hadron [4]. The model inputs are the nuclear mean fields and the (in-medium) elementary hadron–hadron cross-sections. In the cross-section part, we employ the in-medium cross-sections as given in ref. [5] that are parametrized with the corresponding experimental data for $\sqrt{s} \leq 3.5$ GeV with all nucleon resonances up to a mass of 2 GeV. The choice of this parameter $\sqrt{s} \leq 3.5$ GeV implies that it fits the transverse mass spectra of protons in central Au+Au collisions at AGS energies. For higher

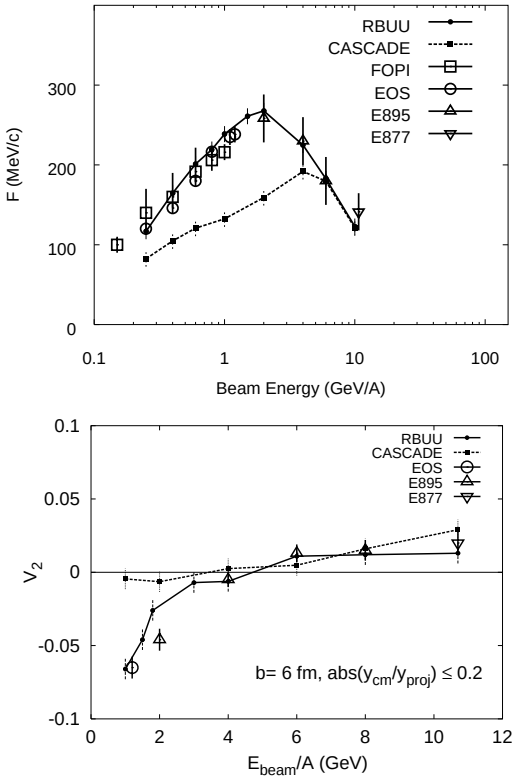

Figure 2. The upper panel shows the sideward flow F as a function of the beam energy for Au+Au collisions at $b = 6$ fm from the RBUU calculations. The solid line results for the parameter set RBUU, the dotted line for a CASCADE calculation with $\sqrt{s} = 3.5$ GeV. The lower panel shows the elliptic flow v_2 of protons, the lines are the same as the upper panel.

energies the Lund string formation and fragmentation model [6] are employed. This is similar to the approach of hadron-string-dynamics (HSD) model [4]. In the relativistic transport approach the nuclear mean field contains both vector- and scalar-potentials U^{ν} and U^{S}, respectively, that depend on the nuclear density and momentum. These potentials are parametrized by the form factors at the vertices [7,8]. These parameters are obtained by fitting (for more details see [7]) the Schrödinger equivalent potential to Dirac phenomenology for intermediate energy proton–nucleus scattering [3].

3. Results

In figure 1 we show the proton transverse mass spectra in a central collision of Au+Au at 11.6 A·GeV ($b < 3.5$ fm) for $\sqrt{s} = 2.6$ GeV (dotted histograms) and 3.5 GeV (solid histograms) in comparison to the experimental data of the E802 Collaboration [9]. A CASCADE calculation (crosses) is shown additionally for $\sqrt{s} = 3.5$ GeV to demon-

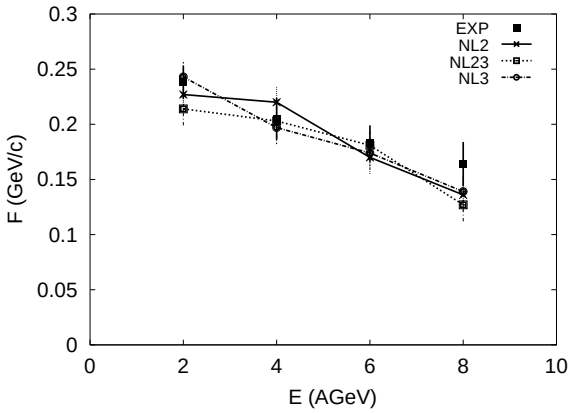

Figure 3. The flow F as a function of beam energy for Au+Au collisions at $b = 6$ fm for the parameter sets NL2 (—), NL23 ($\cdots$) and NL3 (-·--·-). The experimental data (∎) are from the E895 Collaboration.

strate the effect of the mean-field potentials which lead to a reduction of the transverse mass spectra below 0.3 GeV and a substantial hardening of the spectra. As expected, the transverse mass spectrum is softer for smaller $\sqrt{s}$ due to the larger number of degrees of freedom in the string model relative to the resonance model. From the above comparison with the experimental transverse mass spectra for protons in figure 1 we fix $\sqrt{s} \approx 3.5$ GeV; this implies that binary final baryon channels dominate in our transport model up to $\sqrt{s} \approx$ 3.5 GeV which corresponds to a proton laboratory energy $T_{\rm lab}$ of about 4.6 GeV.

In the upper panel of figure 2 the transverse flow F [7,8] is displayed in comparison to the data collected in ref. [10] for Au+Au systems. The solid line (RBUU with $\sqrt{s} = 3.5$ GeV) is obtained with the scalar and vector self energies and the dotted line (CASCADE with $\sqrt{s} = 3.5$ GeV) corresponds to CASCADE calculations. We observe that the solid line is in good agreement with the flow data at all energies. The sideward flow shows a maximum around 2 A·GeV for Au+Au and decreases continuously at higher beam energy ($\geq$ 2 A·GeV) without showing any explicit minimum [11]. This is due to the fact that the repulsive force caused by the vector mean field decreases at high beam energies.

The elliptic flow for protons [7,8] for $|y_{\rm cm}/y_{\rm proj}| \leq 0.2$ is shown in the lower panel of figure 2 as a function of the incident energy for Au+Au collisions at $b = 6$ fm. The flow parameter v_2 changes its sign from negative at low energies ($\leq$ 5 A·GeV) to positive at high energies ($\geq$ 5 A·GeV). We observe that the solid line is in good agreement with data, where the data points are taken from ref. [12].

For completeness, we display the flow F as a function of beam energy in figure 3 for the parameter sets NL2 (solid line) and NL23 (dotted line) along with NL3 (dot–dashed line). These sets are compared to the data from ref. [1] (full squares). We employ similar form factors in NL2 and NL23 parameter sets and the cut-off parameters are determined by fitting the Schrödinger equivalent potential (see details in ref. [8]). From this figure we notice that all parameter sets are roughly compatible with the data. Only at 2 A·GeV the data more clearly favor a 'stiff' EoS as denoted by NL3. The reasonable description of the transverse flow F at 4–8 A·GeV by all parameter sets is attributed to the fact that the momentum dependence of the scalar and vector mean fields is roughly the same. However,

χ^2 analysis favors a 'stiff' EoS at 2 A·GeV while the 4–8 A·GeV data are best reproduced by the 'medium' parameter set NL23. The significant decrease in F at high energies is due to the reduction of vector potential with momentum as pointed out before in ref. [7].

4. Summary

In summary, we have analysed the sideward and elliptic flow from Au+Au at beam energies ranging up to 11 A·GeV in the dynamical simulation model. We found that in order to reach a consistent understanding of the nucleon optical potential up to 1 GeV, the transverse mass distributions of protons at AGS energies as well as the excitation function of sideward and elliptic flows [1,10,12] up to 11 A·GeV, the strength of the vector potential has to be reduced in the RBUU model at high relative momenta and/or densities.

In addition, we have shown the relative role of resonance and string degrees of freedom at AGS energies. By reducing the number of degrees of freedom via high mass resonances one can build up a higher pressure and/or temperature of the 'fireball' which shows up in the transverse mass spectra of protons as well as in the sideward flow [13]. A possible transition from resonance to string degrees of freedom is indicated by our calculations at invariant baryon–baryon collision energies of $\sqrt{s} \approx 3.5 \pm 0.3$ GeV.

Also, using the different nuclear forces starting from soft, medium and stiff equation of state in the microscopic relativistic transport simulation model, we found that the transverse flow F as a function of energy can be rather well-described in the dynamical transport model by all parameter sets which in turn is attributed to the fact that the momentum dependence of the scalar and vector mean fields is roughly the same. A χ^2 analysis favors a 'stiff' EoS at 2 A·GeV while the 4–8 A·GeV data are best reproduced by the 'medium' parameter set NL23. However, the significance for this trend is very low.

Acknowledgements

The authors would like to thank W Cassing and U Mosel for collaborations.

References

[1] E895 Collaboration: H Liu *et al*, *Phys. Rev. Lett.* **84**, 5488 (2000)
N Herrmann *et al*, *Nucl. Phys.* **A610**, 49c (1996)
E895 Collaboration: P Chung *et al*, *Phys. Rev. Lett.* **86**, 2533 (2001)
E895 Collaboration: J L Klay *et al*, *Phys. Rev. Lett.* **88**, 102301 (2002)
[2] E895 Collaboration: P Chung *et al*, nucl-ex/0112002 (2002)
[3] S Hama, B C Clark, E D Cooper, H S Sherif and R L Mercer, *Phys. Rev.* **C41**, 2737 (1990)
[4] W Cassing and E L Bratkovskaya, *Phys. Rep.* **308**, 65 (1999)
[5] M Effenberger, E L Bratkovskaya and U Mosel, *Phys. Rev.* **C60**, 044614 (1999)
[6] B Nilsson-Almqvist and E Stenlund, *Comp. Phys. Comm.* **43**, 387 (1987)
B Anderson, G Gustafson and Hong Pi, *Z. Phys.* **C57**, 485 (1993)
[7] P K Sahu, A Hombach, W Cassing, M Effenberger and U Mosel, *Nucl. Phys.* **A640**, 493 (1998)
P K Sahu, W Cassing, U Mosel and A Ohnishi, *Nucl. Phys.* **A672**, 376 (2000)
[8] P K Sahu and W Cassing, *Nucl. Phys.* **A712**, 357 (2002)

[9] L Ahle *et al*, *Phys. Rev.* **C57**, R466 (1998)
[10] H Liu *et al*, *Nucl. Phys.* **A638**, 451c (1998)
[11] D Rischke, *Nucl. Phys.* **A610**, 88c (1996)
[12] C Pinkenburg *et al*, *Phys. Rev. Lett.* **83**, 1295 (1999)
[13] A Hombach, W Cassing, S Teis and U Mosel, *Euro. Phys. J.* **A5**, 157 (1999)